Azobenzenes for photonic network applications: Third-order nonlinear optical properties

L. BRZOZOWSKI, E. H. SARGENT
Department of Electrical and Computer Engineering, University of Toronto, 10 King's College Road, Toronto, Canada, M5S 3G4
E-mail: lukasz.brzozowski@utoronto.ca

We review the third-order nonlinear performance of pseudo-stilbene type azobenzenes with an eye to application in ultrafast optical signal processing. We discuss mechanisms responsible for the nonlinear response of the azobenzenes. By aggregating experimental data and theoretical trends reported in the literature, we identify five characteristic regions of optical nonlinear response. Analyzed with respect to Stegeman figures of merit, pseudo-stilbene type azobenzenes show promise for ultrafast optical signal processing in two spectral regions, one lying between the main and two-photon absorption resonances, and the other for wavelengths longer than the two-photon absorption resonance.

1. Introduction

Growing demand for the exchange of information in commerce, education, health, government, security, and entertainment creates immense need for transmission bandwidth [1]. Optical fiber provides a suitable medium in which it is possible to reach tremendous transmission rates over long distances using a combination of wavelength- and time-division multiplexing. Optical devices such as arrayed waveguide gratings, micro-electro-mechanical systems (MEMS), fiber Bragg gratings, erbium-doped fiber amplifiers, and isolators are used to multiplex and demultiplex signals, perform coarse switching, amplify pulses, and control the direction of light flow [2].

At present, important, functionally complex operations such as regeneration, reshaping, retiming, and packet routing are carried out electronically. Optical pulses must be converted to electrical signals, processed in the electronic domain, and then converted back to the optical domain. Both the process of optical-electronic-optical conversion, and also the electronic signal processing itself, give rise to bottlenecking at switching and regeneration nodes in present-day optical high-capacity networks. The ability to perform information processing operations entirely within the optical domain would eliminate the need for opto-electrical-opto conversion. The speed of electronic devices would no longer limit network throughput: optical signal processing, in contrast with electronics, may provide subpicosecond switching periods [3].

In an optical switch, light interacts with light by means of a nonlinear material [4]. In materials that exhibit a third-order (Kerr) nonlinearity [4], the effective index of refraction of the material varies in proportion with the local optical intensity I:

$$n = n_0 + n_2 I \tag{1}$$

where n_0 is the linear part of the index and n_2, most often expressed in cm^2/W, is the nonlinear optical Kerr coefficient. A wide range of signal processing devices which rely on Kerr materials have been demonstrated [3, 5–11].

In order for a third-order nonlinear material to be useful in optical signal processing devices it must simultaneously satisfy the following conditions:

1. The excitation time of the nonlinear effect must be less than the pulse width and the sum of the excitation and the relaxation times must be shorter than the pulse spacing.
2. The effect of linear absorption must be weak compared to the effect of nonlinearity. Stegeman quantifies this condition in terms of the figure of merit W [8].

$$W = \frac{\Delta n}{\alpha_0 \lambda} > 1 \tag{2}$$

where $\Delta n = n_2 I$ is the induced index change, α_0 is the linear absorption (expressed in units of inverse length) and λ is the wavelength of light (units of length). Δn is evaluated as I approaches the saturation intensity I_{sat}, at which the rate of increase of refractive index drops noticeably below a linear dependence on intensity.

3. The effect of two-photon absorption must be weak compared to the nonlinear effect. Stegeman quantifies this condition using the figure of merit T [8]:

$$T = \frac{2\beta_2 \lambda}{n_2} < 1 \tag{3}$$

where β is the two-photon absorption coefficient (cm/W).

Conditions 2 and 3 ensure that the nonlinear phase shift $\Delta\phi^{NL} = 2\pi n_2 IL/\lambda$, where L is the length of the

material, reaches 2π before the intensity decays 1/e of its input value as a result of absorption. Phase shifts of this order are required for optical switching devices such as the nonlinear Fabry–Perot interferometer and the nonlinear directional coupler [7].

Although nonlinear optics has been pursued over more than two decades, the field has yet to converge upon a core set of materials which suit the needs of devices for all-optical signal processing [8].

Both organic and inorganic materials have been employed in third-order nonlinear optics. Organic polymeric materials exhibit promising features for all-optical devices. Organic materials exhibit significant fast nonlinearities and low absorption across the visible and infrared spectral regions [12]. They are readily processible into thin-film waveguide structures [13, 14] and do not, in general, rely on a high degree of perfection in ordering or purity to manifest their desired properties. The molecules which make up organic materials provide a tremendous range of structural, conformational, and orientational freedom for exploration with the aid of novel synthetic chemistry, resulting in flexible modification and optimization of linear and nonlinear properties [14].

The pseudo-stilbene type azobenzene organic nonlinear dyes [15–46] represent one particularly promising class of organic nonlinear materials. Various research groups have studied linear and nonlinear properties of azobenzene polymers. Experimental results suggest that, over certain spectral regions, Stegeman figures of merit, as well as response speed requirements for optical signal processing, will be satisfied.

2. Nonlinear properties of azobenzenes

2.1. Theoretical description

The structure of the pseudo-stilbene type azobenzene molecule is depicted in Fig. 1. It consists of an azo group –N═N– between two benzene rings, and push-pull donor and acceptor groups on the opposite sides of the benzene rings [47, 48]. For simplicity, we refer to the pseudo-stilbene type azobenzenes simply as azobenzenes.

Three principal mechanisms lie at the origin of the optical Kerr nonlinearity in azobenzenes: electronic nonlinearities, trans-cis photoisomerization, and thermal effects.

2.1.1. Electronic nonlinearity

Electronic nonlinearities arise from either population redistribution or distortion of electronic clouds. Electronic effects are classified depending on their proximity to absorption resonances. After absorbing a photon, a molecule undergoes a transition from the ground state to the excited state. During such a transition, the dipole moment of the molecule changes. When the change in polarization is dramatic, resonant electronic effects may be of large magnitude. The excitation time of resonant effects is on the subpicosecond time scale. However, as a result of a much slower decay time to the ground state, the recovery time is much longer. Because of large linear absorption, operation near resonance would result a poor first Stegeman figure of merit (W). In addition, absorption, which results in heating and ultimately thermal damage, limits the allowable duty cycle.

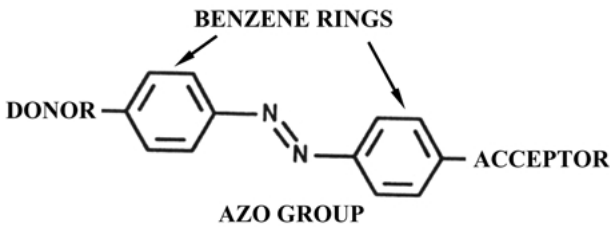

Figure 1 Molecular structure of pseudo-stilbene type azobenzene molecule: the azo group, two benzene rings, donor and acceptor groups.

Azobenzenes exhibit a fundamental absorption maximum (around 400 to 500 nm) and a two-photon absorption (2PA) maximum (at twice the wavelength of the fundamental resonance).

At frequencies far from absorption maxima, molecules exhibit a nonresonant electronic nonlinearity. The optical field induces a dipole moment with response times theoretically estimated to be as short as 10^{-16} s [49]. As will be shown in the experimental section the magnitude of nonresonant electronic nonlinearities is much lower than that of resonant effects. However, negligible absorption far off the resonance allows for Stegeman conditions to be fulfilled.

The electronic response of the azobenzenes may be partially explained with reference to a two-level model wherein a single resonant frequency is considered. This model provides further guidance as to where, relative to a resonance frequency, the most desirable response is to be expected. Comparing expressions for linear and nonlinear absorption with the expression for Kerr nonlinearity suggests that the best figures of merit do not lie half-way between the single- and two-photon absorption resonances [50]. In fact, operating at a wavelength closer to one of the resonances should result in a better nonlinearity-to-absorption ratio. In addition, in order to obtain shorter switching lengths in nonlinear optical devices, larger absolute values of n_2 are required. This again favors spectral regions closer to the resonances. A two-level model also predicts that the third-order electronic nonlinearity should be positive for wavelengths lower than the main resonance, negative in between the resonance, and positive for wavelengths after the 2PA resonance [49].

2.1.2. Trans-cis photoisomerization

Photoisomerization also gives rise to a third-order nonlinearity in azobenzenes [47]. Light of frequency near the main absorption resonance causes the azobenzene molecule to change from the trans to the cis configuration, as illustrated in Fig. 2. During this process, the distance between the two carbons from which the acceptor and donor groups extend reduces from about 0.9 nm to 0.55 nm. This results in a drastic reduction in the molecule's dipole moment, which reduces the material's polarizability providing a large negative nonlinearity of the order $10^{-8}\,\mathrm{cm^2/W}$ to $10^{-11}\,\mathrm{cm^2/W}$ [30].

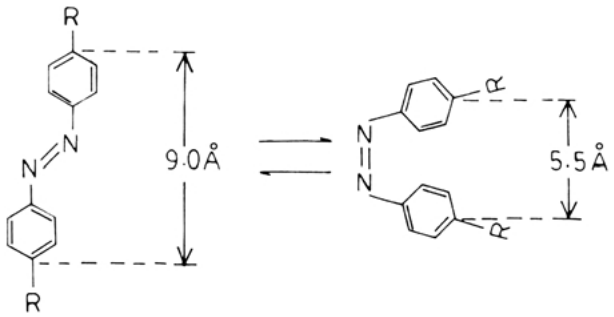

Figure 2 Trans-cis photoisomerization. Following resonant absorption, the azobenzene molecule changes its configuration, resulting in a decreased dipole moment. Reprinted with permission from Yugui Wang *et al*., *J. Chem. Phys.* **103**(13) (1996) 5357.

Wang *et al*. [22] discuss trans-cis photoisomerization dynamics with reference to azobenzene energy levels as shown in Fig. 3. In the absence of light, azobenzene molecules are in the trans configuration in the lowest singlet state S_0. Upon resonant irradiation, molecules absorb light and undergo a transition to the excited state of the trans isomer, S_1. From S_1 the molecule decays to triplet state T_1. From T_1 the molecule can either decay back to S_0 (forbidden, and therefore slow, decay), or to T_1', which is the lowest triplet state of the cis isomer. Trans-cis photoisomerization results in the latter case. Because the energy difference between T_1 and T_1' is of the order of kT, where k is the Boltzmann constant and T temperature, the rate of the transition $T_1 \rightarrow T_1'$ increases with temperature [51, 52]. Once the molecule is in the T_1' state, it may return to the T_1, or alternatively decay to S_0', the ground state of the cis isomer. From S_0' it may be excited to S_1' and decay $S_1' \rightarrow T_1'$ from which it may backward isomerize. However, the rate of $T_1' \rightarrow S_0'$ is much faster ($\sim 400\,\mu s$) than $T_1 \rightarrow S_0$ ($\sim 60\,ms$), so that a molecule in T_1' is most likely to decay to S_0' rather than backward isomerize. In the absence of radiation, the cis isomer decays via thermal relaxation to the trans isomer ($S_0' \rightarrow S_0$). The time required to photoisomerize has been estimated to be less than one picosecond [18] while the decay constant of this relaxation ranges from ms [18] to minutes for methyl orange [22].

Although the magnitude of the nonlinearity due to the trans-cis photoisomerization is very large, several factors tend to limit the usefulness of this mechanism in all-optical switching. Because photoisomerization takes place around the main resonance, absorption is significant and experimental results suggest that Stegeman figures of merit will not be satisfied [18]. The slow relaxation time of backward isomerization would impose severe limits on the duty cycle.

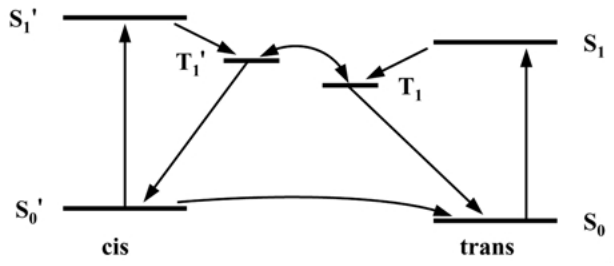

Figure 3 Energy level diagram of the pseudo-stilbene type azobenzene molecule. Following resonant absorption in the trans configuration, the azobenzene molecule photoisomerizes to the cis isomer. Reprinted from book ''Azo Functional Polymers, Functional Group Approach in Macromolecular Design'' by Sudesh Kumar, Fig. 5.1 from page 93, with permission from Technomic Publishing Co., Inc., copyright (1992).

Though the utility of trans-cis photoisomerization in real-time nonlinear optical signal processing is uncertain, the phenomenon has been applied elsewhere. Trans-cis photoisomerization has been found to be the prerequisite for the formation of surface-relief gratings (SRG) formed in azobenzenes films illuminated by an interference pattern using light near the material resonance [53–55].

2.1.3. Thermal effects

Thermal nonlinearities arise from a change in the refractive index with increasing temperature due to optical absorption [56]. In azobenzenes the thermal nonlinearity originates from a decrease in optical density of the medium resulting in the negative index change. Thermal nonlinearities are strong nonlinear effects. However, due to long excitation and relaxation times (usually μs but in extreme cases as high as 1 ms and minutes, for excitation and relaxation respectively, depending on the sample's thermal properties), this type of nonlinearity is not applicable for high-bandwidth optical signal processing.

2.1.4. Sample preparation

To realize bulk and thin-film samples, azobenzene dyes are embedded in a polymer matrix (guest-host arrangement) or attached covalently to a polymer chain (side-chain arrangement). Among the most commonly used polymers are poly(methlymethacrylate) (PMMA) and poly(1,4-phenylenevinylene) (PPV). The side-chain configuration results in more thermally stable and more strongly nonlinear properties than the guest-host approach [27, 28]. For a specific azobenzene-polymer pair there exists a specific concentration of azobenzene in the polymer for which the nonlinear response will be optimized at a given wavelength [15, 21]. For example, Muto *et al*. [21] found that for the disperse red 1 side-chain linked to PMMA, the nonlinear response at 532 nm increases with increasing concentration up to 1 wt % (by weight) of DR1 in PMMA and decreases for larger concentrations. Typical concentration range between 0.5 wt % and 20 wt % [18, 21, 25].

Galvan-Gonzales *et al*. [26] analyzed the thermal and environmental stability of disperse red 1. It was predicted that optically induced oxidation, which degrades the nonlinear properties of azobenzenes, prevents DR1 from offering stability over 10 years at continuous 1-mW illumination in a typical channel waveguide. Other groups studied the effect of continuous UV radiation on azobenzenes, which has been found to result in breakage of the double bond in –N═N– [15] and to cause photo-oxidation [26]. These studies suggest that future nonlinear optical devices may have to be sealed in a hermetic package as with the majority of present-day high-performance optoelectronic devices.

2.2. Experimental

Third-order nonlinearity of azobenzenes and related performance parameters have been studied extensively through experiment [15, 17–21, 23, 25, 31, 35, 36, 41]. Two characterization methods have been employed: Z-scan and degenerate four wave mixing (DFWM).

We show in Fig. 4a schematic for the Z-scan experimental apparatus. A laser beam is focused and the transmittance through the sample is recorded as the position of the sample is varied relative to the focal length of the lens. A reference beam detector is used to monitor the fluctuations of the input laser beam. Z-scan is performed in two configurations: with and without an aperture on the detector. Measurement with an aperture in place allows determination of the sign and magnitude of the Kerr coefficient, while measurement with no aperture allows determination of the sign and magnitude of two-photon absorption [56].

DFWM involves mixing of four optical waves, all at the same frequency. As indicated in Fig. 5 there are three input waves: two high-intensity pump beams and a weak probe beam. The two input beams create a grating that scatters the third input wave. From the dependence of the intensity of the scattered output (conjugate) beam on pump beam intensity the magnitude of the Kerr coefficient is calcuated. DFWM allows easier analysis of the temporal characteristics of the nonlinear mechanism than Z-scan but does not reveal the sign of the nonlinearity [56].

The published results of measurements of nonlinear properties of azobenzenes are summarized in Table I under the following headings: azobenzene name, polymer name, laser source type and parameters (wavelength, pulse width, repetition rate), nonlinear characterization method, Kerr coefficient (n_2), two-photon absorption coefficient (β), linear absorption coefficient (α), Stegeman figures of merit W and T, saturation intensity, maximum value of index change obtained, and origin of nonlinearity. The table is incomplete. It includes only those data provided in the published reports cited. In Fig. 6, we show the diagrams of the molecular structure of azobenzenes from Table I.

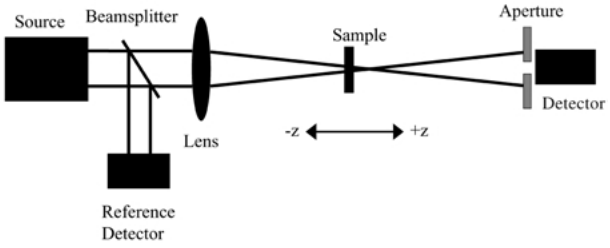

Figure 4 Schematic of experimental apparatus for Z-scan experiment. Nonlinear sample is translated parallel to the beam along the focal point.

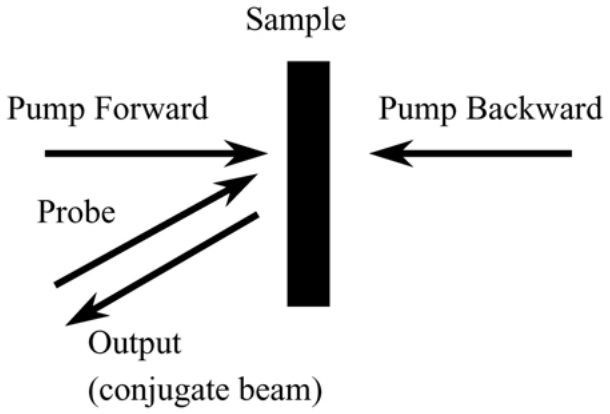

Figure 5 Arrangement for the degenerate four wave mixing experiment. Interference of three input beams gives rise to conjugate beam. The intensity of the conjugate beam is recorded as pump intensity is varied.

Electronic effects far from resonance result in n_2 of the order $10^{-14}\,\mathrm{cm}^2/\mathrm{W}$ to $10^{-12}\,\mathrm{cm}^2/\mathrm{W}$ and very low absorption losses. Trans-cis photoisomerization gives rise to large negative nonlinearities with magnitudes of up to $10^{-8}\,\mathrm{cm}^2/\mathrm{W}$, but large absorption results in poor Stegeman figures of merit (values in the range $W \sim 0.2$ and $T \sim 10$, which are not acceptable for device applications) [18]. Thermal effects result in the largest negative nonlinearities and index changes but, as discussed previously, their slow character prevents utilization in optical information processing.

A few results defy these trends. Misoguti *et al*. [41] obtained $n_2 = 1.8 \times 10^{-14}\,\mathrm{cm}^2/\mathrm{W}$ for disperse red 1 at 532 nm with 70 ps pulses [41]. Strong absorption at this wavelength is otherwise expected to result in trans-cis isomerization for picosecond pulses and orders of magnitude larger Kerr coefficients [18, 21]. Zhang *et al*. [23] reported a positive value for the thermal nonlinearity although the shape of the Z-scan curve suggests negative n_2 [23]. Fei *et al*. [31] and Tomov *et al*. [36] also give a positive thermal Kerr coefficient, a result which should likely be interpreted as a magnitude of the Kerr coefficient since DWFM was employed.

3. Discussion

The spectrum of azobenzene optical behavior may be divided into five regions of characteristic response. These five characteristic regions are illustrated in Fig. 7.

1. Wavelengths below the main resonance (usually below ~ 300 nm): Weak electronic nonlinearity with moderate absorption.

The nonlinearity is weak (at most $10^{-12}\,\mathrm{cm}^2/\mathrm{W}$) and the linear absorption moderate. Azobenzenes are unlikely to find application in optical signal processing in this spectral region.

2. Wavelengths near resonance (~ 300 nm to ~ 600 nm): Strong nonlinear effect due to photoismerization, accompanied by large absorption.

Trans-cis photoisomerization results in Kerr coefficients as high as $10^{-8}\,\mathrm{cm}^2/\mathrm{W}$ near the absorption maximum. The response time of the tran-cis-induced nonlinearity is subpicosecond, but the recovery time is very slow. This restricts the feasibility of this region to applications in which the pulses used are short but repetition rates are low. Limited experimental evidence suggests that Stegeman figures of merit ($W \sim 0.2$ and $T \sim 10$) are unsatisfactory in this spectral region [18].

3. Wavelengths between main and two-photon absorption resonances (~ 600 to ~ 900 nm): Fast electronic nonlinearity, negligible linear absorption, moderate two-photon absorption.

TABLE I Nonlinear material properties for azobenzene dyes

No.	Ref.	Material	Source	n_2(cm^2/W)	β (cm/W)	I_{sat}(W/cm^2)	Δn_{max}	α (cm^{-1})	W	T	Origin
1	25	DR1/PMMA side chain, 20%	Ti:Saph, 820 nm, 150 fs	-6.2×10^{-13} Z-scan	1.7×10^{-10}	—	—	—	—	0.04	e
2	25	DR1/PMMA side chain, 1%	Ti:Saph, 875 nm, 150 fs	—	—	—	—	0.2	—	—	—
3	20	DR1/PPV side chain	Nd:Yag, 1850 nm, 8 ns, 10 kHz	1.9×10^{-13}	—	—	—	—	—	—	e
4	20	DR1/PPV side chain	Nd:Yag, 1907 nm, 8 ns, 10 kHz	5.6×10^{-14}	—	—	—	—	—	—	e
5	17	NMHAA	DFBL, 497 nm, 0.5 ps	-1.5×10^{-13}	—	—	—	30	—	—	e
6	41	DR1	Nd:Yag, 532 nm, 70 ps, 100 Hz	1.8×10^{-14} Z-scan	—	—	—	1.5	—	—	—
7	18	DR1/PMMA side chain	Nd:Yag, 560 nm, 20 ps, 10 Hz	-1.8×10^{-9} Z-scan	1.6×10^{-4}	64×10^{6}	0.12	10048	0.2	9.7	TC
8	18	DR1/PMMA side chain	Nd:Yag, 570 nm, 20 ps, 10 Hz	-5×10^{-9} Z-scan	4.6×10^{-4}	13×10^{6}	0.065	6095	0.19	10.4	TC
9	18	DR1/PMMA side chain	Nd:Yag, 580 nm, 20 ps, 10 Hz	-3×10^{-10} Z-scan	2.5×10^{-5}	190×10^{6}	0.042	3451	0.2	9.6	TC
10	18	DR1/PMMA side chain	Nd:Yag, 590 nm, 20 ps, 10 Hz	-5×10^{-11} Z-scan	—	—	—	1856	—	—	TC
11	18	DR1/PMMA side chain	Nd:Yag, 600 nm, 20 ps, 10 Hz	-2×10^{-11} Z-scan	—	—	—	927.3	—	—	TC
12	18	DR1/PMMA side chain	Nd:Yag, 610 nm, 20 ps, 10 Hz	-1×10^{-11} Z-scan	3.1×10^{-7}	—	—	470	—	3.8	TC
13	21	DR1/PMMA 1%	Nd:Yag, 532 nm,	-2.4×10^{-8}	—	—	—	—	—	—	TC
14	19	DR1	640 nm,	-9.3×10^{-9} Z-scan	—	—	—	—	—	—	Th
15	23	DR1	Dye, 640 nm, cw	$(-)1.7\times10^{-6}$ Z-scan	—	—	—	—	—	—	Th
16	23	NMHAA	Dye, 640 nm, cw	$(-)4.8\times10^{-8}$ Z-scan	—	—	—	—	—	—	Th
17	31	Azodye 1	HeNe, 633 nm cw	$(-)1.7\times10^{-5}$ DFWM	—	—	—	—	—	—	Th
18	35	MO/polyimide	Ar Ion, 488 nm cw	-5.7×10^{-6}	—	—	—	—	—	—	Th
19	36	Sudan G	633 nm cw	$(-)4\times10^{-5}$	—	—	0.007	0.35	—	—	Th

DR1, disperse red 1; PMMA, poly(methylmethacrylate; PPV, poly(1,4-phenylenevinylene; DFBL, distributed feedback laser; NMHAA, 4-nitro, 4′-(N-methyl, N-hecadecyl) amino azobenzene; cw, continuous wave; MO, methyl orange; MR, methyl red; (−) negative nonlinearity expected; e, electronic; TC, trans-cis; Th, thermal.

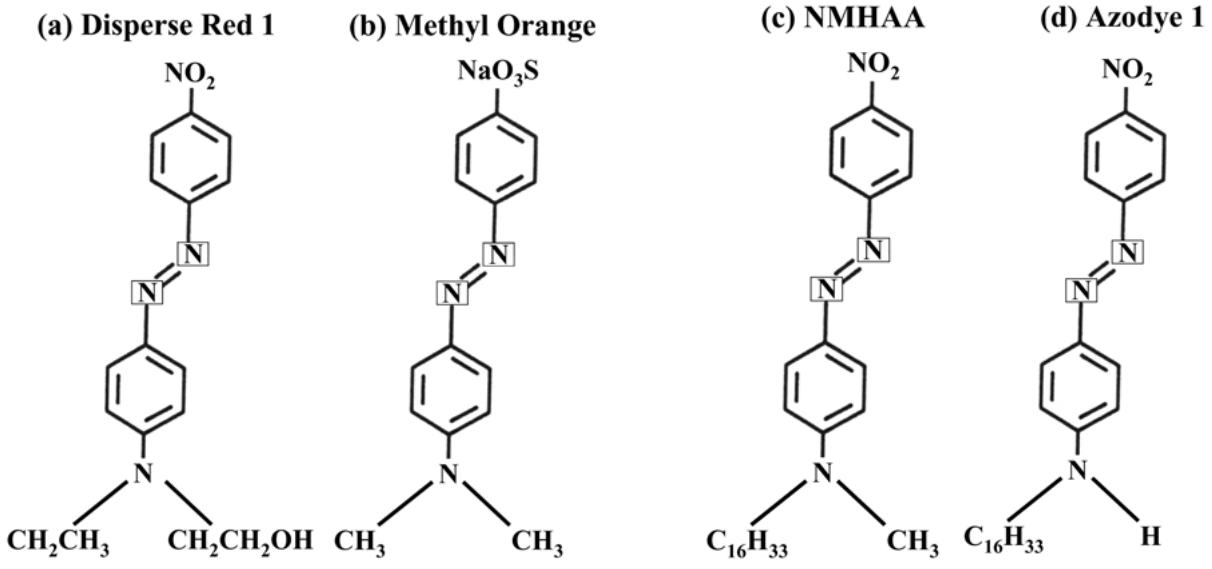

Figure 6 Molecular structure of nonlinear azobenzene dyes (a) disperse red 1, (b) methyl orange, (c) NMHAA, (d) an azobenzene dye from Fei *et al.* [31].

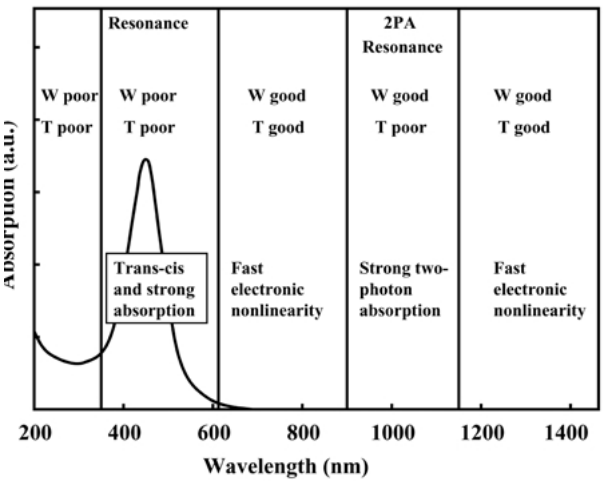

Figure 7 Typical absorption spectrum and generalized nonlinear properties of a pseudo-stilbene type azobenzene molecule. The Stegeman figures of merit are indicated in each of the characteristic spectral regions.

In this spectral region, Kerr coefficients lie between 10^{-14} cm^2/W and 10^{-12} cm^2/W. The fast response time is compatible with processing of optical pulses which are spaced closely in time (e.g. small number of picoseconds). Experimental data suggest that the Stegeman conditions will be satisfied in this spectral region. Linear absorption is negligible and an acceptably small value of 0.04 was obtained for the two-photon absorption figure of merit T [25].

4. Wavelengths near the two-photon absorption resonance (usually between ~ 900 and ~ 1200 nm): Fast electronic nonlinearity and two-photon absorption peak.

No trans-cis photoisomerization has been reported in this region. The electronic contribution to the Kerr coefficient is greater than in Region 3, but the trade-off due to the two-photon absorption prevents the Stegeman figures of merit from being acceptable for photonic switching applications.

5. Wavelengths longer than two-photon absorption resonance (usually above ~ 1100 nm): Fast electronic nonlinearity, weak linear and two-photon absorption.

Fast virtual electronic transitions result in nonlinearity in the range of 10^{-14} cm^2/W to 10^{-12} cm^2/W. The lack of linear and two-photon absorption in this spectral region permits the Stegeman conditions to be satisfied. Ultrafast response times enable extremely high repetition rates in which the benefits of an all-optical approach are realized. This regime coincides with wavelengths used in fiber-optic communications systems (1300–1600 nm), making azobenzenes particularly attractive for all-optical signal processing applications. The possibility of linear absorption losses arising from higher-order photon absorption and vibrational overtones [57, 58] are a cause for concern and merit further experimental investigation.

4. Conclusions

The nonlinear properties of pseudo-stilbene type azobenzene dyes have received significant attention over the past 10 years in view of the urgent need for efficient, functional optical signal processing for ultra-high-speed communications and networking. As the principal conclusion of the present work we put forth that azobenzenes show distinct promise in such applications in two spectral regions, one lying between the main and two-photon absorption resonances, and the other for wavelengths longer than two-photon absorption resonance.

In general, there is a lack of corroborated data elaborating the optical properties of azobenzenes over all spectral regions of scientific and application-oriented interest. To evaluate azobenzenes with a view to optical information processing applications, nonlinear behavior must be elucidated across pertinent regimes of optical wavelength, pulse width, peak intensity, and duty cycles. The evolution of nonlinear figures of merit with increasing dye concentration requires experimental characterization. Degradation processes should be examined with a view to building a suitable environment in which azobenzene-based optical signal processing devices may provide longevity in their novel function.

References

1. E. COTTER, J. K. LUCEK and D. D. MARCENAC, *IEEE Commun. Mag.* **34** (1997) 90–95.
2. R. RAMASWAMI and K. N. SIVARAJAN, ''Optical Networks, A Practical Prespective'' (Morgan Kaufmann Publishers Inc., 1998).
3. P. W. SMITH, *Bell Syst. Tech. J.* **61** (1982) 1975–1983.
4. B. E. A. SALEH and M. C. TEICH, ''Fundamentals of Photonics'' (John Wiley & Sons Inc., 1991).
5. P. W. E. SMITH and L. QIAN, *Bell Syst. Tech. J.* **15** (1999) 28–33.
6. P. W. E. SMITH, in 1998 International Conference on Applications of Photonic Technology III: Closing the Gap between Theory, Development, and Applications, **3491** (SPIE, 1998) 3–8.
7. P. W. E. SMITH, in Nonlinear Optical Properties of Advanced Materials **1852** (SPIE, 1993) 2–9.
8. G. I. STEGEMAN, in Nonlinear Optical Properties of Advanced Materials, **1852** (SPIE, 1993) 75–89
9. L. BRZOZOWSKI and E. H. SARGENT, *J. Opt. Soc. Am.* **17** (2000) 1360–1365.
10. L. BRZOZOWSKI and E. H. SARGENT, *IEEE J. Quantum Electron.* **36** (2000) 550–555.
11. L. BRZOZOWSKI and E. H. SARGENT, *ibid.* **36** (2000) 1237–1242.
12. N. J. LONG, ''Organometallic Compounds for Nonlinear Optics – The Search for Enlightenment!'' Angewandte Chemie, International Edition (English) **34** (1995) 21–38.
13. I. LIAKATAS, C. CAI, M. BÖSCH, C. B. M. JÄGER and P. GÜNTER, *Appl. Phys. Lett.* **76** (2000) 1368–1370.
14. P. N. PRASAD and D. J. WILLIAMS, ''Introduction to Nonlinear Optical Effects in Molecules and Polymers'' (John Wiley and Sons, 1991) pp. 3, 4, 14.
15. C. EGAMI, Y. SUZUKI, O. SUGIHARA, N. OKAMOTO, H. FUJIMURA, K. NAKAGAWA and H. FUJIWARA, *Appl. Phys. B* **64** (1997) 471–478.
16. C. EGAMI, Y. SUZUKI, O. SUGIHARA, H. FUJIMURA and N. OKAMOTO, *Jpn. J. Appl. Phys.* **36** (1997) 2902–2905.
17. F. DONG, E. KOUDOUMAS, S. COURIS, Y. SHEN, L. QIU and X. FU, *J. Appl. Phys.* **81** (1997) 7073–7075.
18. R. RANGEL-ROJO, S. YAMADA, H. MATSUDA and D. YANKELEVICH, *Appl. Phys. Lett.* **72** (1998) 1021–1023.
19. C. R. MENDONÇA, M. M. COSTA, J. A. GIACOMETTI, F. D. NUNES and S. C. ZILIO, *Electron. Lett.* **34** (1998) 116–117.
20. C. B. YOON, J. I. LEE and H. K. SHIM, *Synth. Met.* **84** (1997) 273–274.
21. S. MUTO, T. KUBO, Y. KUROKAWA and K. SUZUKI, *Thin Solid Films* **322** (1998) 233–237.
22. Y. WANG, J. ZHAN, J. SI, P. YE, X. FU, L. QIU and Y. SHEN, *J. Chem. Phys.* **103** (1996) 5357–5361.

23. Z. X. ZHANG, W. QIU, E. Y. B. PAN, P. S. CHUNG and Y. Q. SHEN, *Synth. Met.* **84** (1997) 273–274.
24. X. LIU, G. XU, J. SI, P. YE, Z. LI and Y. SHEN, *J. Appl. Phys.* **88** (2000) 3848–3852.
25. S. YAMAKAWA, K. HAMASHIMA, T. KNOSHITA and K. SASAKI, *Appl. Phys. Lett.* **72** (1998) 1562–1564.
26. A. GALVAN-GONZALES, M. CANAVA, G. I. STEGEMAN, R. TWIEG, T. C. KOWALCZYK and S. LACKRITZ, *Opt. Lett.* **24** (1999) 1741–1743.
27. S. BAUER, W. REN, S. YILMAZ, W. WIRGES, W.-D. MOLZOW, R. GEHRARD-MULTHAUPT, U. OERTEL, B. HÄNEL, L. HÄUSSLER and K. L. H. KOMBER, *Appl. Phys. Lett.* **63** (1993) 2018–2020.
28. P. PANTELIS, in ''Conducting Polymers and Their Application'' (IEE, 1992) pp. 4/1–4.
29. M. IVANOV, T. TODOROV, L. NIKOLOVA, N. TOMOVA and V. DRAGOSTINOVA, *Appl. Phys. Lett.* **66** (1995) 2174–2176.
30. V. M. CHURIKOV and C. C. HSU, *ibid.* **77** (2000) 2095–2097.
31. H. FEI, Z. WEI, Q. YANG, Y. CHE, Y. SHEN, X. FU and L. QIU, *Opt. Lett.* **20** (1995) 1518–1520.
32. A. A. R. A. YUSOF, S. V. O'LARY and G. R. MITCHELL, *Opt. Commun.* **169** (1999) 333–340.
33. Y. YANG, H. FEI, Z. WEI, Q. YANG, G. SUN and L. HAN, *J. Lumin.* **66** (1996) 133–135.
34. Y. YANG, H. FEI, Z. WEI, Q. YANG, G. SUN and L. HAN, *Opt. Commun.* **123** (1996) 189–194.
35. K. ZLATANOVA, P. MARKOVSKY, J. SPASSOVA and G. DANEV, *Opt. Mater.* **5** (1996) 279–283.
36. A. V. TOMOV, A. I. VOITENKOV and A. V. KNOMCHENKO, *Tech. Phys.* **43** (1998) 249–250.
37. L. M. BLINOV, M. V. KOZLOVSKY, K. N. DN M. OAZKI and K. YOSHINO, *Jpn. J. Appl. Phys.* **35** (1996) 5405–5410.
38. G. KLEIDEITER, Z. SEKKAT, M. KREITER, M. D. LECHNER and W. KNOLL, *J. Molec. Struct.* **52** (2000) 167–178.
39. M. SKOWRONEK, I. ROTERMAN, L. KONIECZNY, B. STOPA, J. RYBARSKA, B. PIEKARSAK, A. GÓRECKI and M. KRÓL, *Comput. Chem.* **24** (2000) 429–150.
40. S. DELYSSE, P. RAIMOND and J.-M. NUNZI, *Chem. Phys.* **219** (1997) 341–351.
41. L. MISOGUTI, C. R. MENDONÇA and S. C. ZILIO, *Appl. Phys. Lett.* **74** (1999) 1531–1533.
42. M. IWAMOTO, Y. MAJIMA, H. NARUSE and K. IRIAMA, *J. Appl. Phys.* **72** (1992) 1631–1636.
43. C. EGAMI, Y. SUZUKI, T. UEMORI, O. SUGIHARA and N. OKAMOTO, *Opt. Lett.* **22** (1997) 1424–1426.
44. K. SAITO, Y. YAMAMURA, K. KIKUCHI and I. IKEMOTO, *J. Phys. Chem. Solids* **56** (1995) 849–857.
45. M. TERAZIMA, *Chem. Phys. Lett.* **230** (1994) 87–92.
46. W.-R. CHO, V. RICCI, T. PLISKA, M. CANAVA and G. I. STEGEMAN, *J. Appl. Phys.* **86** (1999) 2941–2944.
47. S. KUMAR, ''Azo Functional Polymers'' (Technomic Publishing Co. Inc., 1992), pp. 92, 93.
48. H. RAU, in ''Photochemistry and Photophysics'', **2** (CRC Press, 1990) 120–141.
49. R. W. BOYD ''Nonlinear Optics'' (Academic Press Limited, 1992), pp. 172, 350.
50. D. C. HANNA, M. A. YARATICH and D. COTTER, ''Nonlinear Optics of Free Atoms and Molecules'' (Springer-Verlag, 1979) pp. 34, 60, 61.
51. S. MALKIN and E. FISHER, *J. Phys. Chem.* **66** (1962) 2482–2486.
52. H. STEGEMEYER, *ibid.* **66** (1962) 2555–2560.
53. F. L. LABARTHET, P. ROCHON and A. NATANSOHN, *Appl. Phys. Lett.* **75** (1999) 1377–1379.
54. C. BARRETT, P. L. ROCHON and A. L. NATANSOHN, *J. Chem. Phys.* **109** (1998) 1505–1516.
55. J.-A. HE, S. BIAN, L. LI, J. KUMAR, S. K. TRIPATHY and L. A. SAMUELSON, *Appl. Phys. Lett.* **76** (2000) 2233–2235.
56. R. L. SUTHERLAND, ''Handbook of Nonlinear Optics'' (Marcel Dekker, Inc., 1996), pp. 327–408.
57. A. V. BAKLANOV, M. ALDENER, B. LINDGREN and U. SASSENBERG, *J. Chem. Phys.* **112** (2000) 6649–6655.
58. D. M. TURNBULL, H. G. KJAERGAARD and B. R. HENRY, *Chem. Phys.* **195** (1995) 129–141.

Received 2 April
and accepted 25 June 2001